Optimization of the thermochromic glazing design for curtain wall buildings based on experimental measurements and dynamic simulation

Marco Arnesano [a,*], Giuseppe Pandarese [b], Milena Martarelli [b], Federica Naspi [b], Kargal L. Gurunatha [c], Christian Sol [c], Mark Portnoi [c], Francisco V. Ramirez [c], Ivan P. Parkin [d], Ioannis Papakonstantinou [c], Gian Marco Revel [b]

[a] Università Telematica eCampus, 22060 Novedrate (CO), Italy
[b] Dipartimento di Ingegneria Industriale e Scienze Matematiche, Università Politecnica delle Marche, 60131 Ancona, Italy
[c] Photonic Innovations Lab, Department of Electronic & Electrical Engineering, University College London, WC1E7JE London, United Kingdom
[d] Department of Chemistry, University College London, WC1E7JE London, United Kingdom

ARTICLE INFO

ABSTRACT

Thermochromic (TC) glazing could provide a significant reduction of energy consumption in curtain wall buildings. However, each application requires a design tailored to building's specifications. This paper proposes a complete approach for designing TC glaze based on building energy simulation starting from the production of thin thermochromic layers and the measurements of their optical properties by means of a customized spectrophotometer. The main focus of this work is to identify the optimal TC optical response that minimises the building energy consumption. Energy simulations have been performed for a virtual mock-up set at two locations with different climates, Italy and Poland. A set of profiles, each one determining thermochromic properties in terms of switching temperature, range of solar transmittance and transition speed, have been created with a fine step of temperature (2 °C) and used to simulate different scenarios. The outcome of the optimization provided the optimal properties to achieve the right balance between cooling energy reduction and heating energy increase due to the application of the thermochromic layer, in comparison to a standard clear glass. The fine step in switching temperature allowed to accurately estimate the subtle differences for the two different climates (25 °C Italy, 24–26 °C Poland). The highest impact has been found for the Italian location with a maximum reduction of total energy consumption of 22.8%. This was achieved with a thermochromic switching at 25 °C, with fast transition and range of transmittance between 0.1 (switched state) and 0.5 (normal state), which is a not extreme behaviour.

1. Introduction

A gradual increase in the energy consumption with concomitant increase in industrialization brought much attention into development of energy conservation and energy harvesting strategies. According to the United Nations, 35–40% of the world's energy consumption and approximately one-third of greenhouse gas emissions can be attributed to the built environment and is anticipated to increase steadily (Riffat and Mardiana, 2015; Santamouris, 2014). Therefore, there is an extensive demand to construct more sustainable energy saving architectures by making full use of renewable energies such as solar energy. Central heating, ventilation, and air conditioning are the main sources of energy consumption and have been estimated to account for about 7% of all

anthropogenic CO_2 emissions (Intergovernmental Panel on Climate Change, 2014). Moreover, windows are known as one of the least energy efficient components of buildings, where heat transmittance and insulation inefficiency are responsible for 15–22% of a building's energy loss (Hee et al., 2015). Thus, switchable glazing (Lorenza Bianco et al., 2017; L. Bianco et al., 2017; Fazel et al., 2016; Kuhn, 2017) has emerged as a promising technique for the development of next generation smart windows that display energy saving characteristics by regulating the incoming solar radiation. This is achieved mainly by change in optical response with respect to the surrounding climate or user input. The two main adaptive approaches employed for switchable glazing are active electrochromic technology, in which the change in optical properties is initiated by an applied electrical stimulus and passive thermochromic

technology, where the material reacts to the heat resulting in optical property modulation (Tällberg et al., 2019). The major difference between the two methods is that the change in light transmission properties of the former is obtained by applying an external voltage, whereas the latter performs the state change only when ambient temperature rises above a critical threshold (Long and Ye, 2014a).

Over the years, thermochromic glazing materials gained increased importance due to their capacity to reversibly transform from a transparent state to an opaque state with respect to external and internal thermal variation. In this technology, vanadium dioxide (VO_2) has drawn widespread attention as a promising energy conserving material due to its particular phase transition feature (Cui et al., 2018). The peculiar reversible metal-insulator transition (MIT) of VO_2 (M1) phase with remarkable near infrared (NIR) switching at critical temperature T_C (typically about 68 °C) makes it an excellent candidate for thermochromic smart windows (Berglund and Guggenheim, 1969). The basic principle of VO_2 based thermochromic glazing is that above Tc, in its high temperature rutile VO_2 (R) state, the material becomes highly opaque and reduces NIR transmission significantly, while keeping relatively high transmittance in visible spectrum. Below Tc, in its monoclinic VO_2 (M) state, it allows desired solar gain for passive heating during cold days. Several studies have been conducted to implement VO_2 based glazing to improve building energy efficiency and indoor comfort based on the simulation of typical building rooms (residential, offices, etc.) indicating the high potential of the material (Hee et al., 2015). Notably, the effects of three kinds of VO_2 glazing, at different critical temperature and radiation properties (transmittance, reflectance, absorption), on the passive performance of a residential room were simulated by Long et al. and their efficiency was calculated in terms of objective indexes defined by the authors (Long and Ye, 2014b). The proposed indexes were the energy saving equivalent parameter, connecting the thermal state parameter with a hypothetical energy consumption, and the energy saving index, used to evaluate the performance of building components or materials. Moreover, they also simulated the combined effect of the VO_2 film and double-glazed window that possesses two advantages, i.e. ability to dynamically control the solar radiation into the building, and ability to block the heat from entering (leaving) the building in the summer (winter) (Long et al., 2015). Raicu et al. demonstrated the strong dependence between the optimum switching temperature of thermochromic glazing and the total solar and internal gains of the building (Raicu et al., 2002). While they approximately accounted for the material hysteresis, the effects of the hysteresis slope and transition speed were not studied. However, these are crucial parameters owing to the large area of building windows.

In this paper, the complete performance assessment of the thermochromic glazing in comparison to standard clear glass is presented. In order to investigate this, we optimized a VO_2 thin-film structure (120 nm) showing exceptionally high solar modulation while maintaining high degree of transparency and narrow hysteresis. The optical properties were measured at different temperature conditions. For that scope, a spectrophotometer was equipped with a temperature-controlled sample holder to perform temperature-dependent reflectance measurements. The customized holder allowed the use of a traditional spectrophotometer instead of more complex and expensive instruments (Barron et al., 2015, 2014). After the TC layer's characterization, the effect of thermochromic glazing on building consumption was calculated by performing a dynamic energy simulation considering different solar transmittance curves, where the variables were the switching temperature, the luminous and solar average transmittance value at the VO_2 (R) and VO_2 (M) states and the transmittance transition speed. Results from the dynamic simulation were used to determine the optimal fine tuning of the thermochromic glazing behavior as a function of the outdoor conditions. A virtual mock-up was created using the EnergyPlus simulation engine that has already proved to be applicable in such studies (Saeli et al., 2010).

The final goal of the paper is to present the experience and lessons learnt derived from the EENSULATE project ("Eensulate"), where a methodology for thermochromic performance optimization under different climatic conditions was developed and applied. In particular, the thermochromic layer is intended to be applied to a new VIG (Vacuum Insulated Glass) window for glazed façade to enhance energy performance.

The outcomes of the paper provide original insights about: i) the evaluation of TC impact on building's energy consumptions considering multi-variable configurations, including a 2 °C switching temperature step variation that allows a fine-grained calculation of trade-off curves; ii) the impact of TC layer applied to the VIG technology under two different climates; iii) the application of a low-cost solution to equip a standard spectrophotometer with a temperature-controlled sample holder to be used for TC layer's characterization in terms of both transmittance and reflectance.

The paper is organized as following: Section 2 describes the glazing system that is under investigation, the thermochromic glazing preparation process and the measurement setup for optical characterization. Section 3 describes the virtual mock-up, based on building's energy dynamic simulation, to assess the impact that the thermochromic layer provides on the final energy consumption. Given the flexibility in changing the thermochromic properties, different configurations are assessed with the virtual test bench. Section 4 presents the discussion of results and Section 5 provides guidelines for the thermochromic glazing configuration based on the experimental and numerical assessment presented in the initial sections of the paper.

2. Methods and materials

2.1. The Eensulate glazing system

The Eensulate project aims to develop a glazing system solution for envelope insulation to bring existing curtain wall buildings to "nearly zero energy" standards. The system consists of a wall module where the thermal insulation is provided by a lightweight and thin double pane vacuum glass and a spandrel filled with highly insulating mono-component and environmentally friendly spray foam. To improve the insulation performance, the glass integrates a thermo-tuneable coating allowing for dynamic solar gain control. General scheme of the glazing unit is shown in Fig. 1.

2.2. Thermochromic glazing preparation

Vanadium pentoxide (V_2O_5, 99.6%), oxalic acid ($H_2C_2O_4$, 99%), anhydrous ethanol (C_2H_5OH), and anhydrous isopropanol (IPA) were purchased from Sigma Aldrich and used without further purification. The fabrication of TC glass was carried by spin coating the vanadium precursor on the substrate followed by thermal annealing under vacuum condition. The detailed step by step fabrication procedure is given below and generalized in Fig. 2a together with a picture of the sample produced for the laboratory characterization (Fig. 2b).

2.2.1. Synthesis of vanadium precursor

The vanadium (IV) precursor solution was synthesised as described previously (Sol et al., 2020). Briefly, heating the mixture of V_2O_5 (1.82 g) with oxalic acid (3.78 g) in 10 ml anhydrous ethanol at 80 °C for 12 h result in the reduction of vanadium (V) to form $[VO(C_2O_4)]$ which can be seen visibly with the change in colour from pale yellow to dark blue. Whilst being heated the solution container was connected to a condenser to avoid evaporation and to maintain the solution concentration (c = 2 M). This stock solution was filtered and was diluted further to the desired concentration with anhydrous ethanol for spin coating on the substrate.

2.2.2. Fabrication of vanadium dioxide (VO_2) thin-films

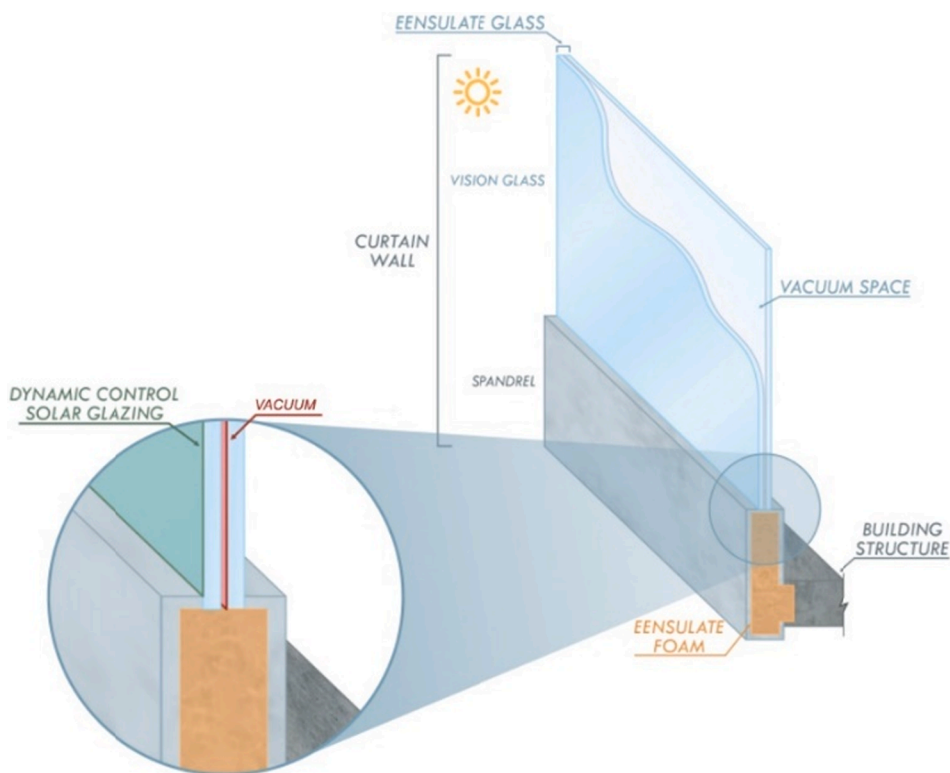The fused silica and quartz substrates were washed thoroughly with

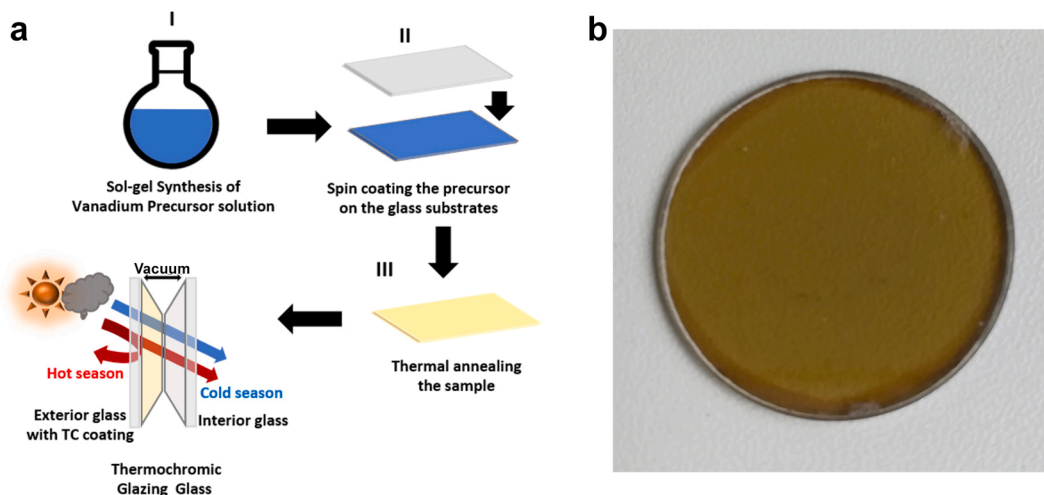Fig. 1. Schematic representation of the prototype glazing unit.

Fig. 2. Scheme of the production process (a) and glass sample with thermochromic coating (b).

acetone and IPA to remove organic impurities and exposed to an oxygen plasma for 1 min to form hydrophilic groups at the surface and ensure improved uniform coating. After the plasma treatment, substrates were spin coated with vanadium oxide precursor at a range of speeds for 30 s (SCS G3 Spin coater) and films were aged in a box furnace at 100 °C for 10 min to remove any remaining solvents. Monoclinic VO_2 was obtained by annealing the spin coated substrate in a tube furnace at 550 °C in vacuum (<10 mbar) for 1 h with the heating and cooling rate of tube furnace set to 20 °C/min. The quality of VO_2 thin-film was analyzed by Raman spectroscopy, performed using an inVia Raman microscope with laser power set to 1% to avoid sample heating. The Raman spectra of VO_2 thin-film show Raman modes at 142, 190, 221, 259, 307, 336, 388, 497 and 612 cm^{-1} and can be readily assigned with that of VO_2(M) phase as reported in the literature (Fig S1) (Shvets et al., 2019). Optical

properties of all samples were measured using Semilab SE-2000 spectroscopic ellipsometer.

The W-doped vanadium dioxide thin film on glass (0.2, 0.5 and 0.7 wt%) was obtained by adding WCl_6 to the vanadium precursor stock solution followed by spin coating on glass substrate and thermal annealing under vacuum at the same condition.

2.3. Experimental assessment of optical properties of the thermochromic glass

Here, we determine the optimal properties of the thermochromic system by means of energy performance dynamic simulations for a building room located in two different geoclimatic areas (Rimini, Italy and Dzierżoniów, Poland, where real demonstration buildings exploited

in the Eensulate project are set) and with the windowed façade having different orientations. To estimate the optical properties to be considered as baseline in the simulation, two types of glazed systems were considered: clear glass and thermochromic glass simply consisting of clear glass coated with a single VO$_2$ layer.

To evaluate the optical performance and hysteresis loop of the thermochromic glass, static measurements of spectral near normal-hemispherical reflectance and transmittance were performed according to standard ASTM E903-2 (ASTM E903-12, Standard Test Method for Solar Absorptance, Reflectance, and Transmittance of Materials Using Integrating Spheres, 2012) in the temperature range from 20 to 90 °C, with ascendant and descendent steps. A JASCO V-670 spectrophotometer equipped with a integrating sphere of 60 mm diameter with thermostat was used for transmittance measurements. The temperature-controlled cell holder was used to maintain the samples at a constant temperature in the range from 20 to 90 °C, with 2 °C resolution. The measurement of transmittance was done performing dark and baseline corrections and working within the 300–2500 nm wavelength region with a spectral resolution of 2 nm.

The JASCO V-670 spectrophotometer equipped with an integrating sphere of 150 mm diameter has been modified for the reflectance measurement by exploiting a self-made, Peltier-controlled heating system. The sample holder and the heating system are shown in Fig. 3.

The transmittance and reflectance spectra, T(λ) and R(λ), measured during an ascending temperature test at the limit temperatures (20 and 90 °C) for both the thermochromic and clear glass are reported as a function of wavelength (λ) in Fig. 4. By processing the spectra at different temperatures, the optical properties of the thermochromic glass and the clear one were calculated in terms of:

– Visible light transmittance (T_{lum}) and reflectance (R_{lum}) obtained by integrating the corresponding spectra in the visible wavelength

range, i.e. 380–780 nm, and normalized with the spectral sensitivity of the human eye response (Smith and Guild, 1931), φ_{lum}, as in Eq. (1) (Taylor et al., 2013).

– Solar transmittance (T_{sol}) and reflectance (R_{sol}) obtained by integrating the corresponding spectra in the solar wavelength range, i.e. solar 300–2500 nm, and normalized with the solar spectral irradiance when the sun is at 37° above the horizon (ASTM G173-03 reference spectra, 2013), AM$_{1.5}$, as in Eq. (2) (Taylor et al., 2013).

$$T_{lum} = \frac{\int_{\lambda=380\ nm}^{780\ nm} \varphi_{lum}(\lambda)T(\lambda)d\lambda}{\int_{\lambda=380\ nm}^{780\ nm} \varphi_{lum}(\lambda)d\lambda} \quad R_{lum} = \frac{\int_{\lambda=380\ nm}^{780\ nm} \varphi_{lum}(\lambda)R(\lambda)d\lambda}{\int_{\lambda=380\ nm}^{780\ nm} \varphi_{lum}(\lambda)d\lambda} \quad (1)$$

$$T_{sol} = \frac{\int_{\lambda=300\ nm}^{2500\ nm} AM_{1.5}(\lambda)T(\lambda)d\lambda}{\int_{\lambda=300\ nm}^{2500\ nm} \overline{AM_{1.5}}(\lambda)d\lambda} \quad R_{sol} = \frac{\int_{\lambda=300\ nm}^{2500\ nm} AM_{1.5}(\lambda)R(\lambda)d\lambda}{\int_{\lambda=300\ nm}^{2500\ nm} \overline{AM_{1.5}}(\lambda)d\lambda} \quad (2)$$

The trends of the four optical parameters defined above as a function of the temperature are reported in Fig. 5a, b for the solar components and Fig. 5c, d for the luminous components. The solid red line was obtained from the tests performed with ascending temperature (heating process) and the dashed blue line from the tests performed with descending temperature (cooling process). As expected, the transmittance modulation occurs only in the solar range, this guaranteeing the same optical behavior in the visible range at any temperature.

The reflectance instead shows a more complex behavior as evidenced by the spectra reported in Fig. 4(b) and also reported in (Gao et al., 2012). It is clear that the reflectance changes with temperature also in the visible range with an opposite trend with respect to the solar range. This is reflected in the luminous and solar reflectance trends in function of temperature, Fig. 5 (b and c).
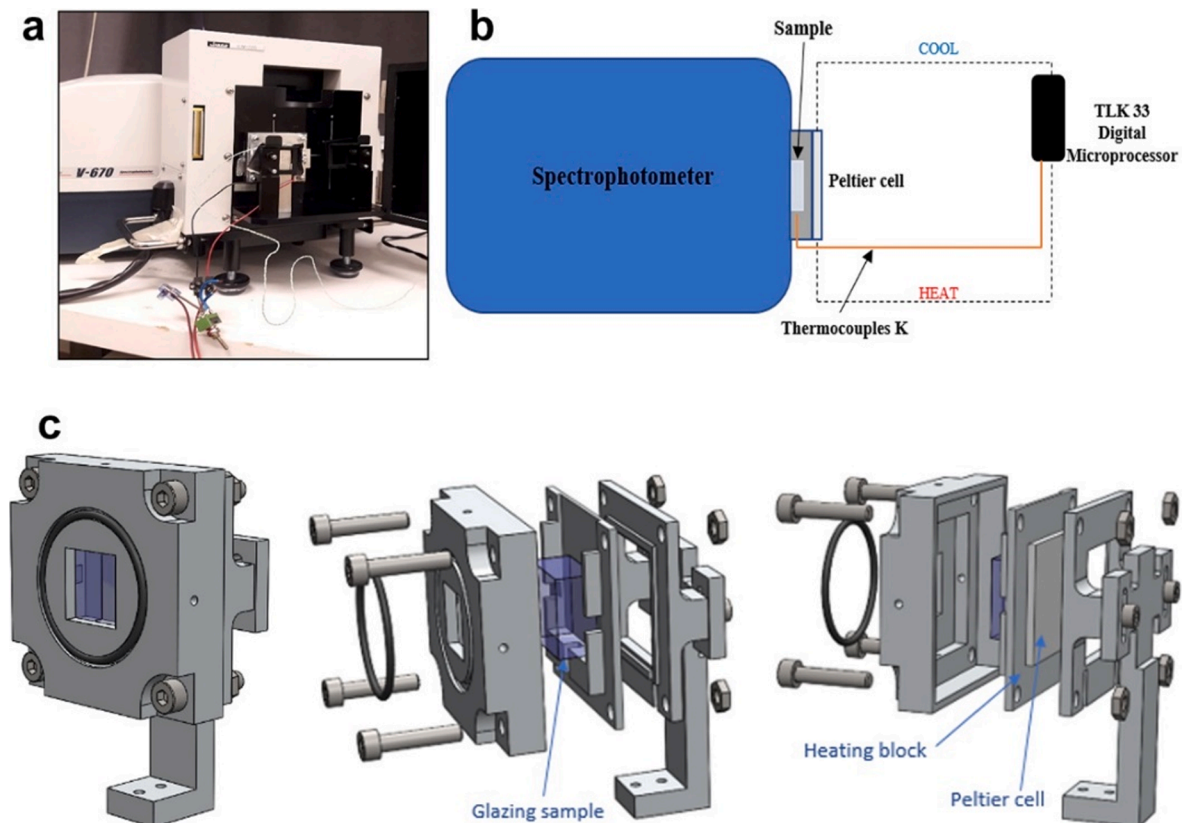

Fig. 3. JASCO V-670 Spectrophotometer (a) with the controlled Peltier heater system for reflectance measurement (b). The cell holder and Peltier-controlled heater (c).
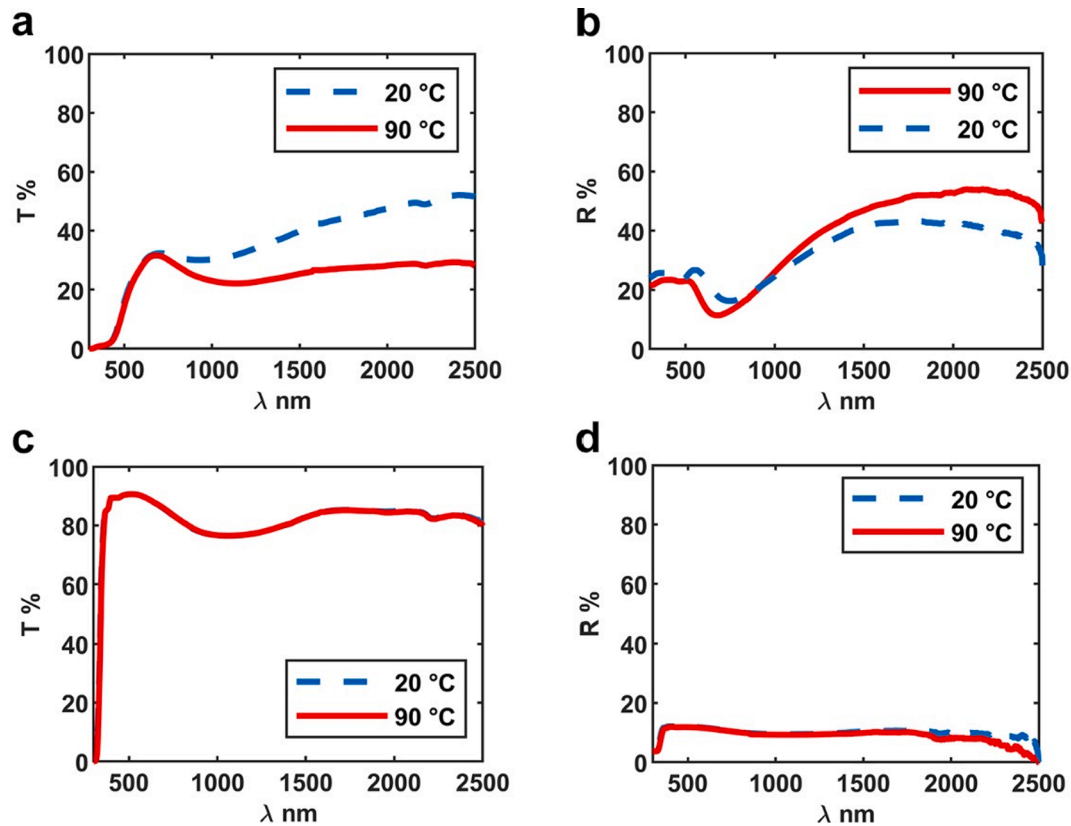
Fig. 4. Transmittance (left) and reflectance (right) spectra of thermochromic coated glass (a, b) and clear glass (c, d) at 20 and 90 °C.

3. Numerical assessment of the impact on buildings' performance

The impact that the TC glass has on buildings performance has been investigated using a virtual mockup. Using such an approach, different configurations of the windows could be investigated with the scope of achieving the optimal one with respect to the geographical location of the building. This section describes the virtual mockup and the outcome of the numerical assessment applied to two different climates.

3.1. Description of the virtual mock-up

The virtual mockup alongside the whole simulation process have been realized using EnergyPlus ("EnergyPlus"), which is a free and open-source building energy simulation program developed by the U.S. Department of Energy. The virtual mock-up (Fig. 6) is a very simple box with a surface of about 50 m² and a heated volume of 150 m³, similarly to what has been done by previous study for thermochromic glazing assessment (Saeli et al., 2010). All the façades were opaque except one which had a glazed surface of 20 m². The stratigraphy and the thermal features of the materials are reported in Table 1. The mock-up was set with office end-use and occupancy, while loads and schedules were applied following the prescription of ASHRAE 2005 Handbook of Fundamentals (ASHRAE Handbook: Fundamentals, 2005) on the basis of the selected end-use. To isolate the effect of the type of glazing, all other surfaces have been set as adiabatic. Similarly, the HVAC system was an ideal system with infinite capacity. Such an ideal system can supply conditioned air to the zone to meet all the load requirements and it does not consume energy.

The weather files used in the simulations were derived from the EnergyPlus weather files database. The selected climates corresponded to the location of the two demo cases of the EENSULATE project. The two locations are Rimini, located in Italy (latitude: 44.03; longitude: 12.62; elevation: 13 m) and Dzierżoniów, settled in Poland (latitude: 50.73; longitude: 16.65; elevation: 261 m). According to Köppen-Geiger climate classification (Kottek et al., 2006), both the locations have a warm temperate climate (i.e. Category Cfb). Since the weather file for Dzierżoniów is not provided by EnergyPlus, Wroclaw (latitude: 51.10; longitude: 17.03; elevation: 124 m) has been selected instead as the nearest available location, being distant of about 60 km. Each simulation covered a duration of one year, with a time-step of 10 min. Table 2 summarizes the main simulation settings.

The objective of the study presented in this section is to evaluate energy performance of the TC glass in comparison to standard clear glass. The EENSULATE project develops a new VIG window for glazed façade that could be composed with or without the thermochromic layer. For this reason, the scope of this study is to assess the impact of the thermochromic layer on building performances with respect to two reference conditions. The first one is a non-VIG and non-thermochromic glasse, consisting of a 4 mm double-glazing with interposed 5 mm of air (4 + 5 + 4), called 'Standard_1' in the rest of the paper. The second reference, called 'Standard_2', is a double-glazing with interposed 5 mm of a custom gas, created specifically to simulate the vacuum. The same gas has also been used for the thermochromic glazing. In fact, EnergyPlus does not allow simulating a vacuum cavity and a thermochromic layer at the same time. To overcome this limitation, a custom gas (called near- vacuum) has been defined. The features of the clear glass and the near-vacuum gas are recapped in Table 3 and Table 4.

The thermochromic glazing has been modelled according to the features described previously with solar transmittance and reflectance curves modelled according to the shape derived from the experimental analysis (Section 2.3). EnergyPlus does not identify the thermochromic as a coating of the glass but as the entire glass having thermochromic properties. Therefore, the glazing is a double-glazing with an exterior thermochromic component (4 mm), an interior clear glass (4 mm) and interposed 5 mm of the near-vacuum gas. Another limitation of the
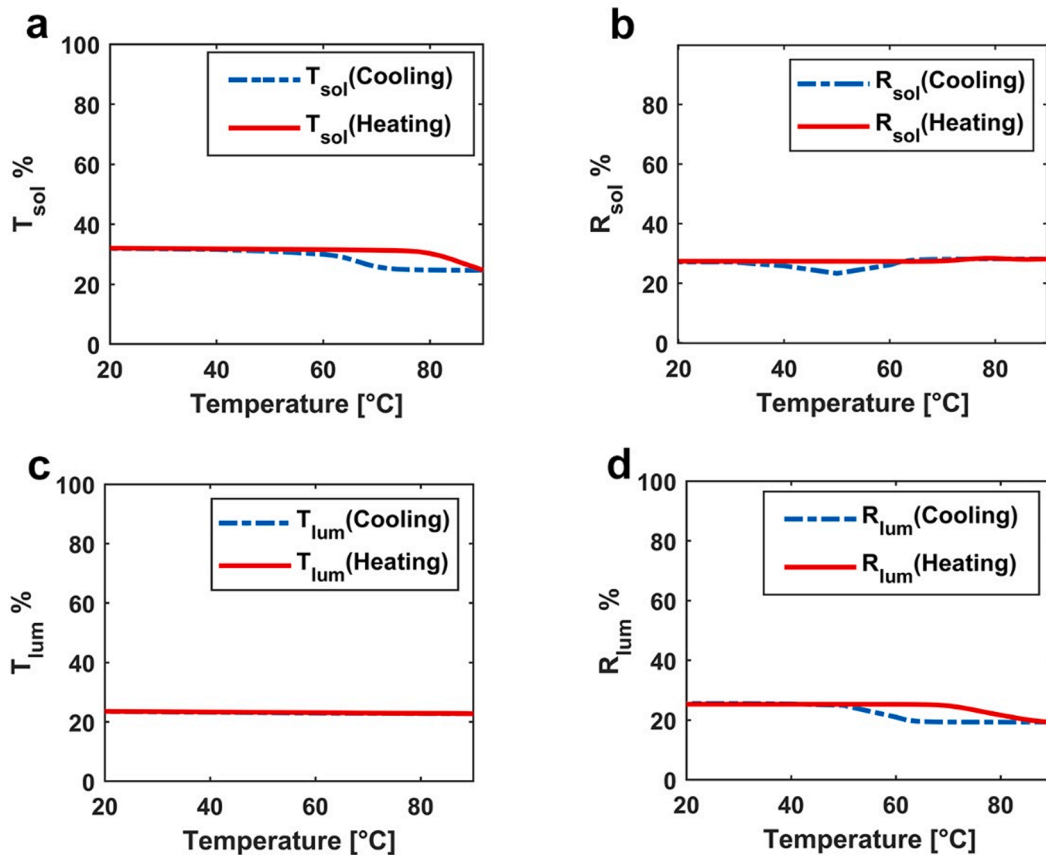
Fig. 5. (a) Solar transmittance, (b) solar reflectance and (c) luminous transmittance, (d) luminous reflectance of thermochromic coated glass during heating (red line) and cooling (blue line) cycle. (For interpretation of the references to colour in this figure legend, the reader is referred to the web version of this article.)
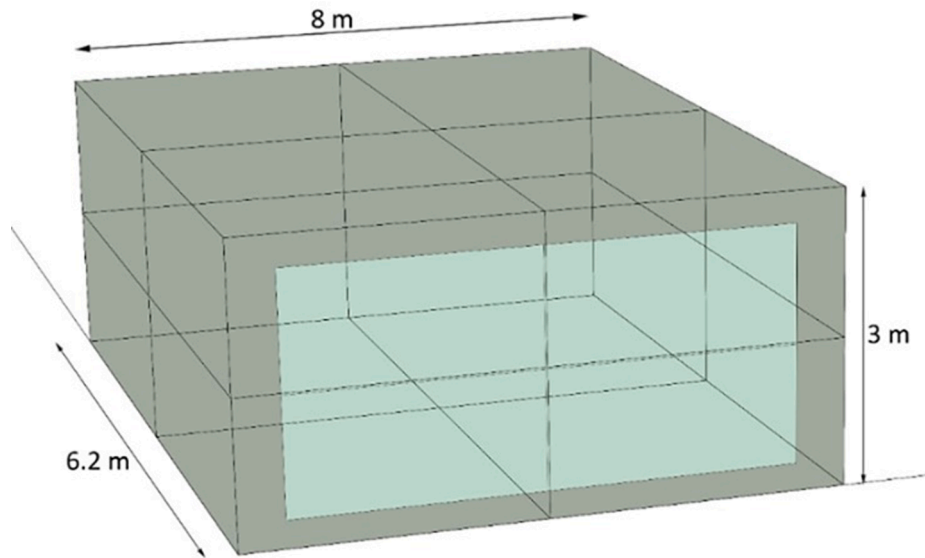

Fig. 6. Sketch of the mock-up.

simulation program is the lack of hysteresis. The special feature the program provides to create thermochromic glazing (i.e. the Thermochromic object) is not integrated with the hysteresis. As a consequence, only the ascent curve has been used to perform the energy simulations. This simplification should not produce large deviations since the distance between the ascent and descent curve is very small. Therefore the hysteresis was not a significant impact on the energy and visual comfort

performance as demonstrated in the literature (Giovannini et al., 2019).

3.2. Simulation of the standard glazing for benchmarking

This Section illustrates the results obtained running the simulations with the two benchmarks. Table 5 and Table 6 present the energy consumptions using the two types of glazing for Rimini and Dzierżoniów,

Table 1
Stratigraphy and thermal features of the materials.

Construction	Material	Thickness (m)	Conductivity (W/mK)	Density (kg/m³)	Specific heat (J/kgK)
Opaque façades	Indoor plaster	0.01	0.58	800	1090
	Concrete blocks	0.2	1.11	800	920
	Expanded polystyrene	0.08	0.036	20	1210
	Outdoor plaster	0.01	0.58	800	1090
Floor	Tiles	0.013	0.057	290	590
	Lightweight concrete	0.05	0.53	1280	840
	Insulation board	0.05	0.03	43	1210
	Heavyweight concrete	0.2	1.95	2240	900
Roof	Indoor plaster	0.01	0.58	800	1090
	Insulation board	0.1	0.03	43	1210
	Lightweight concrete	0.2	0.53	1280	840

Table 2
Simulation settings.

End use	Office
Location	Rimini (Italy) & Dzierżoniów (Poland)
Simulation time-step	10 min
Simulation run period	1 year
Heating set-point (°C)	21
Cooling set-point (°C)	26.7
People (person/m²)	0.05
Lights (W/m²)	11.84
Electric equipment (W/m²)	6.89
Flow per zone floor area (m³/s m²)	0.0002

Table 3
Features of the clear glass.

Optical properties of the clear glass	
Thickness (m)	0.004
Solar transmittance at normal incidence	0.82
Front side solar reflectance at normal incidence	0.074
Back side solar reflectance at normal incidence	0.074
Visible transmittance at normal incidence	0.875
Front side visible reflectance at normal incidence	0.08
Back side visible reflectance at normal incidence	0.08
Infrared transmittance at normal incidence	0
Front side infrared hemispherical emissivity	0.84
Back side infrared hemispherical emissivity	0.84
Conductivity (W/mK)	0.9

Table 4
Features of the near-vacuum custom gas.

Thermal properties of the near-vacuum gas	
Thickness (m)	0.005
Conductivity coefficient (W/mK)	0.00287
Viscosity coefficient (kg/ms)	0.001
Specific Heat coefficient (J/kgK)	0.001
Molecular Weight	20
Specific Heat Ratio	1.001

Table 5
Comparisons of energy performance (Rimini).

Rimini (IT)	Standard_1	Standard_2
Total Energy (kWh/m²)	104.5	95.2
Heating Energy (kWh/m²)	32.7	26.4
Cooling Energy (kWh/m²)	54	51.2
Lighting Energy (kWh/m²)	17.8	17.6

Table 6
Comparisons of energy performance (Dzierżoniów).

Dzierżoniów (PL)	Standard_1	Standard_2
Total Energy (kWh/m²)	104.6	89.9
Heating Energy (kWh/m²)	68.4	54.4
Cooling Energy (kWh/m²)	17.6	16.8
Lighting Energy (kWh/m²)	18.6	18.7

respectively.

As expected, the Standard_2 provides a reduction of the energy consumption, given by the increased thermal insulation of the vacuum layer. Using the baseline simulation, an investigation on the performance of the glass has been carried out in order to understand its behavior in both climates. Table 7 reports a brief statistical analysis of the external glass temperature, including the maximum reached values. Similarly, Fig. 7 depicts the absolute frequency of the temperature reached during the one-year simulation using the Italian (Fig. 7a) and Polish (Fig. 7b) weather files.

Both Fig. 7 and Table 7 highlight that the glazing temperature is mostly distributed between 0 °C and 45 °C for Rimini and between −10 °C and 40 °C for Dzierżoniów. Considering that the application of a thermochromic coating aims at reducing the energy consumption during cooling seasons, only the right side of the temperature distributions is used to select the range of possible transition temperatures of the TC. The virtual mockup serves here to find the thermochromic characteristics providing the optimal balance between heating and cooling energy.

3.3. Simulation of the thermochromic glazing

To investigate the effect of the activation of the TC layer on the energy performance of the mock-up, the solar transmittance curve has been parametrized so to create different shapes according to Table 8. The parameters considered are:

– The minimum solar transmittance reached in the hot state
– The maximum solar transmittance achieved in the cold state
– The switching temperature
– The slope coefficient related to the temperature transition speed.

The reflectance curve shapes have been set from the transmittance ones considering an absorption of 0.1, according to the conservation of

Table 7
Statistics of the external layer temperature.

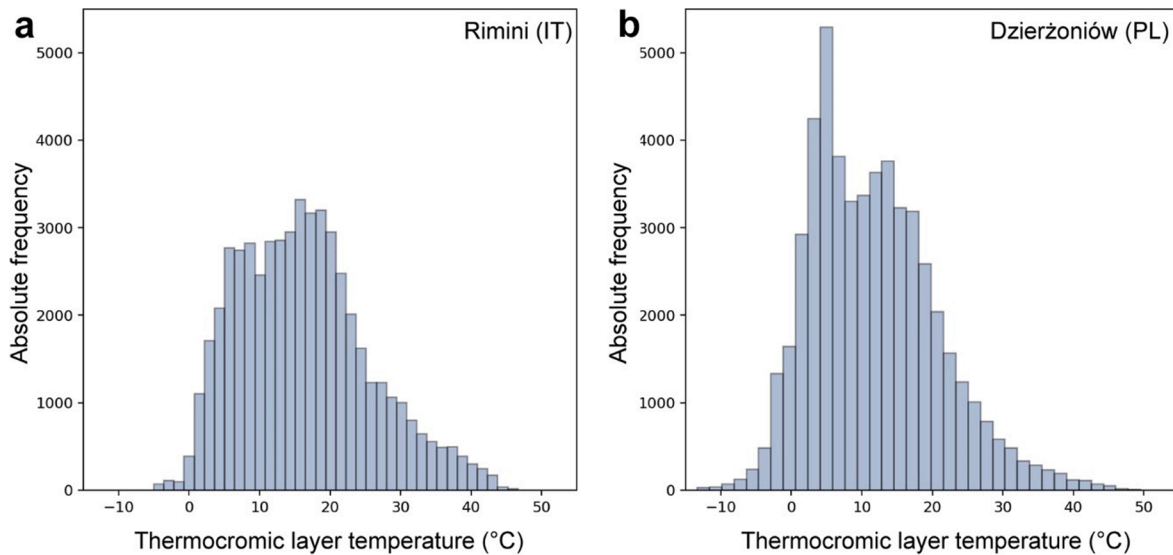| Statistic	Rimini	Dzierżoniów
Maximum (°C)	46.6	49.5
Minimum (°C)	−5	−13.4
Mean (°C)	16.2	11.7
Median (°C)	15.5	10.7

Fig. 7. Absolute frequency of the external layer temperature for a) Rimini and b) Dzierżoniów.

Table 8
Parameters for solar transmittance curve generation.

Parameter	Rimini		Poland		
	Min	Max	Min	Max	Step
Min solar transmittance	0.1	0.3	0.1	0.3	0.1
Max solar transmittance	0.5	0.7	0.5	0.7	0.1
T_{sw} (°C)	25	45	20	40	2
Slope coefficient	0.05	0.2	0.05	0.2	0.075

energy.

Fig. 8 shows an example of curves for one transition range that were derived from the parametrization and were used for the optimization process applied to Rimini. The other transition ranges used for the optimization process present the same shape but shifted down because of the lower transition limits. Curves applied to Poland have the same shape but with different temperature limits. Each curve has been used to run an energy simulation for each orientation of the two geographical locations. The aim of this process is to find the curve with which the TC glass can provide the lowest energy consumptions, considering heating, cooling and lighting energy use.

4. Discussion of results

The simulation results have been compared with the Standard_2 reference glass in order to provide evidence of the positive or negative impact that can be achieved by applying a thermochromic layer to the base VIG glass. Results are presented in the following figures, where each thermochromic configuration is identified by:

- TR MAX-MIN: boundaries of the transmittance range, where the upper limit indicates the transmittance with thermochromic not switched and lower limit the transmittance with switched thermochromic.
- SL: value of the slope coefficient among those enumerated in Table 8.
- Tsw: the switching temperature of the thermochromic layer.

Each graph in Fig. 9 and Fig. 10 shows in a green circle the configuration that turned out to provide the lowest total energy consumption with respect to the reference condition, that is the Standard_2 glazing. Considering the demo case located in Rimini, Table 9 presents the detailed data of energy consumptions of the best performing configuration for each orientation compared.

For all orientations, except the North one, the optimal energy performance was achieved with a thermochromic layer that had a switching temperature of 25 °C and range of transmittance between 50% (not switched) and 10% (switched) with a fast transition speed (slope 0.2 of
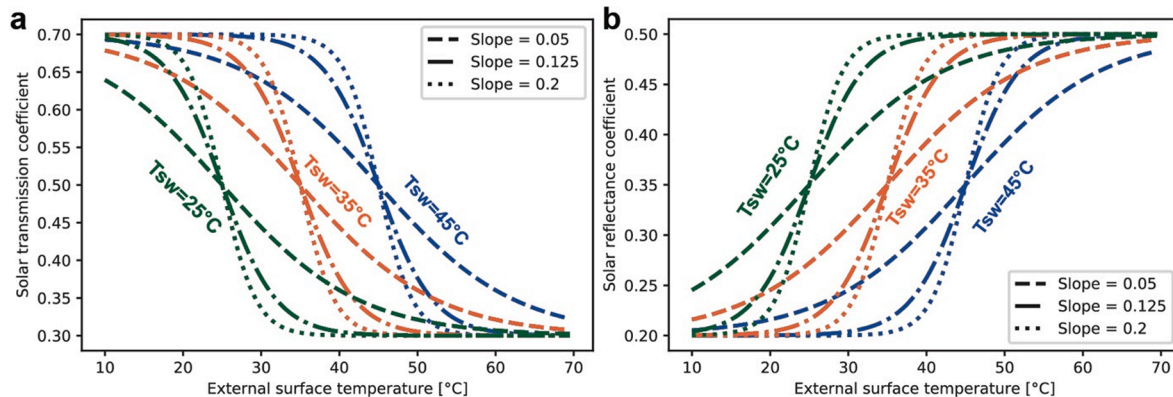

Fig. 8. Curves of (a) solar transmission (b) reflectance (right) referred to a transition range of 0.7 (normal state) and 0.3 (switched state), used for the optimization process.
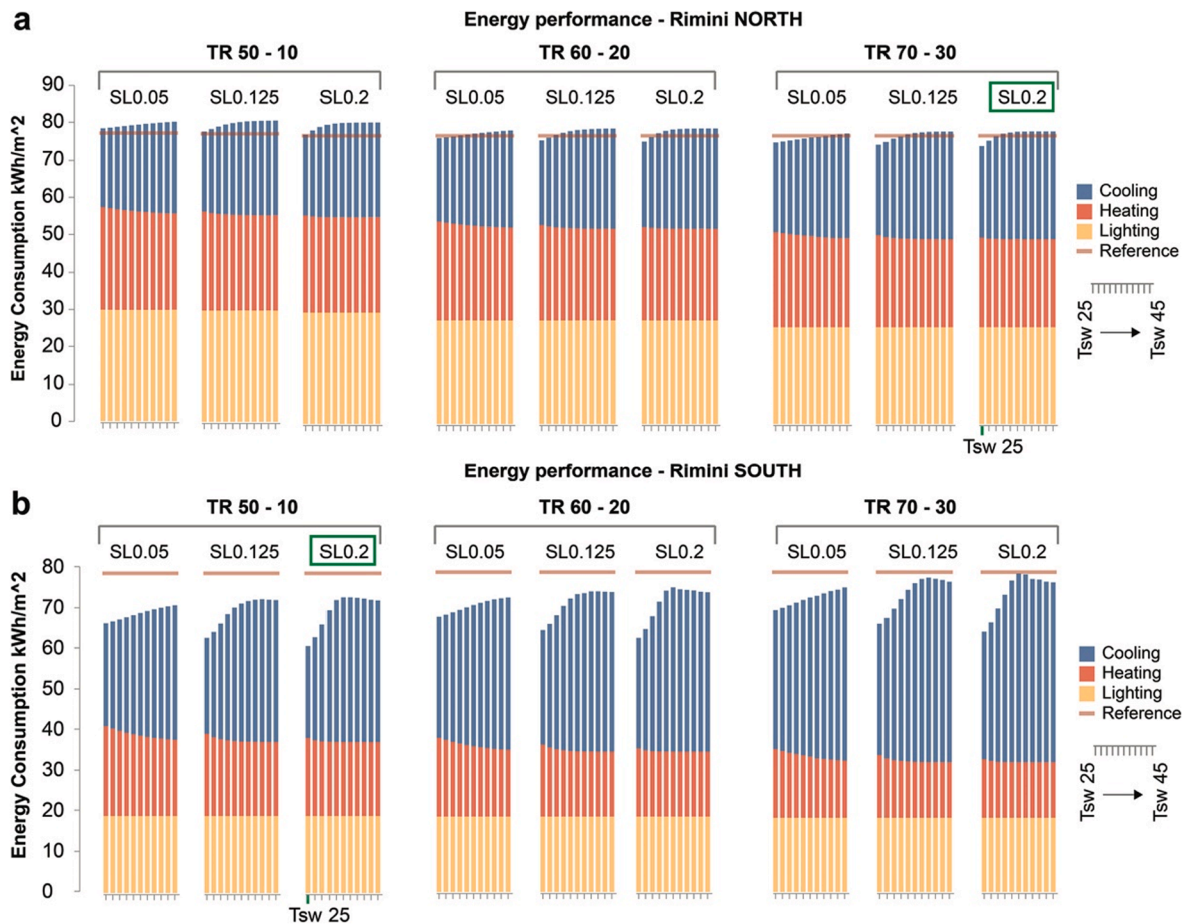
Fig. 9. Energy consumptions for north and south -oriented TC glazed wall located in Rimini, compared to Standard_2 glazing.

the sigmoid curve as shown in Fig. 8). With that configuration, the increase of heating energy, due to the reduced solar gain in winter, is completely compensated by strong reduction of cooling energy. The energy saving achieved with that configuration is always about 20%, completely due to the cooling energy reduction.

Only north-oriented wall results in a different optimal configuration. As expected, this orientation has a lower solar gain in all seasons, so there is a very small compensation of the heating energy increase. In fact, the total energy saving achievable with the north orientation is only 3.6%. Similarly, previous studies demonstrated that using the thermochromic glaze in Mediterranean climate could provide an energy saving between 7% and 35% for 25% window to wall ratio model (Saeli et al., 2010).

Concerning the demo case in Dzierzoniow, only the configuration with TR 70–30, SL 0.2 and Tsw between 24 °C and 26 °C turned out to provide a slight improvement of energy performance. Table 10 depicts the detailed results derived from simulations.

The North orientation does not provide a positive result given by the thermochromic layer. The other orientations register a small reduction of the total energy consumption, but always lower than 5%. The increase of heating consumption due to the thermochromic coating has a higher impact with respect to Mediterranean climates. These results are aligned with previous studies where different climates have been investigated and turned out to provide that thermochromic glass could not be suitable for geographical locations characterized by cold climates as Countries of the North-Eastern Europe (Imbert et al., 2019; Saeli et al., 2010).

Overall, results achieved with the simulation and optimization approach are well aligned with previous works. For example, Costanzo et al. performed a detailed investigation on real and theoretical

thermochromic performances concluding that in hot climates as in Southern Europe an energy saving of 25% is reasonable while in cold climates no more than 5% can be achieved because of the negative effect on heating loads (Costanzo et al., 2016). Also, the review paper presented by Aburas (Aburas et al., 2019) demonstrated that TC windows contribute to heating and cooling energy savings between 5.0% and 84.7%, depending on the climate area. In that study, applications to different zones have been reported from Helsinki to Cairo. Finally, results agree with the ones obtained by Warwick that studied the reduction in energy demand of buildings installing TC windows in relation to the transition temperature and the hysteresis gradient of the TC system having an extreme modulation between hot (15% of transmittance) and cold (80% of transmittance) state (Warwick et al., 2016). Coming back to the present study, the application of a thermochromic layer to the VIG glazing should be evaluated with an economic analysis based on the estimation of the energy cost saving compared to the extra cost for its application.

5. Guidelines for thermochromic glazing configuration

The energy simulation model proved that the thermochromic glazing should have a solar average transmittance modulation (difference between hot and cold state) of about 40% and switching temperature of 25 °C. For that reason, the thickness of VO_2 layer was optimized based on our previous simulation and experimental measurement (Sol et al., 2020). However, the glass coated with a single layer of non-doped VO_2 exhibits instead a modulation of less than 10% and a switching temperature of about 70 °C, as shown in Fig. 4. According to previous studies (Salamati et al., 2019; Warwick et al., 2016), the solution to improve optical performances of the coated glass is to design VO_2
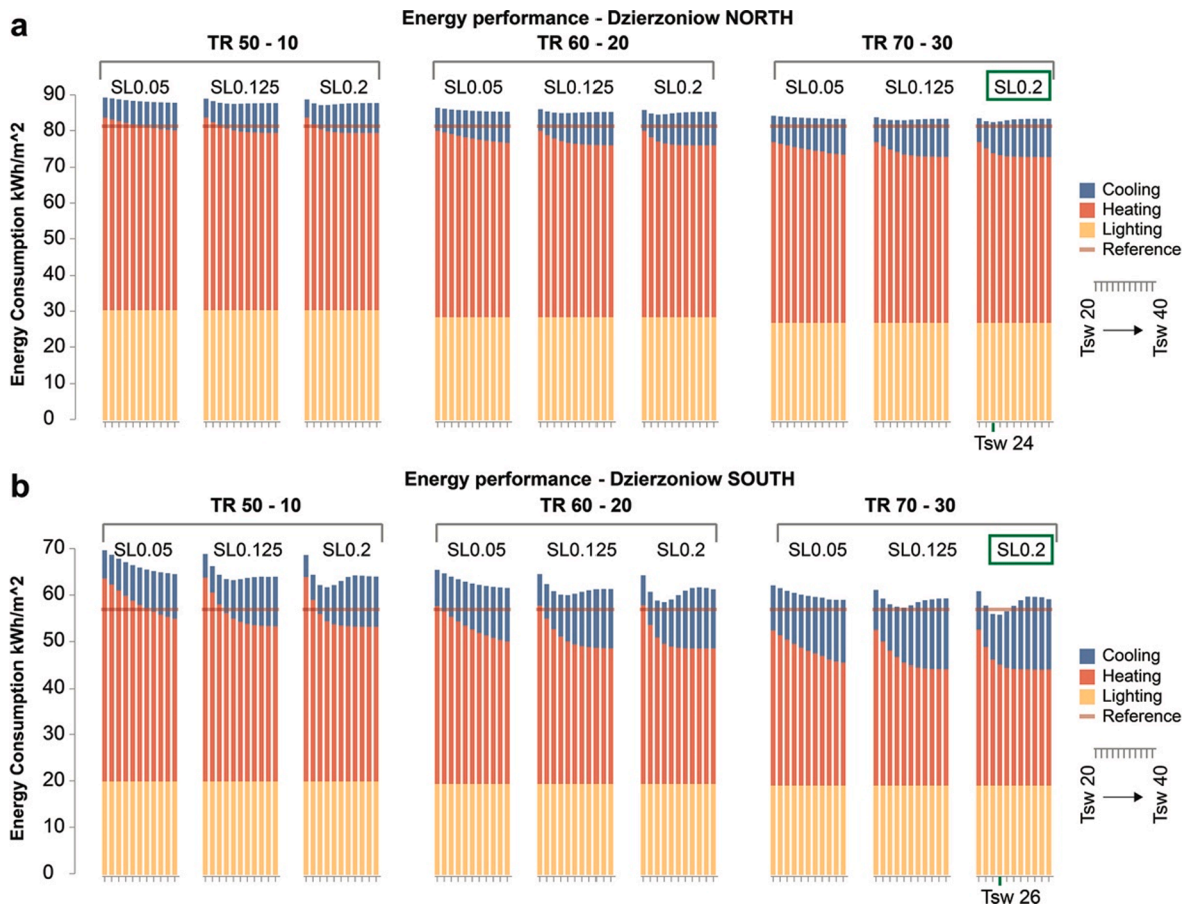
Fig. 10. Energy consumptions for north and south -oriented TC glazed wall located in Dzierzoniow, compared to Standard_2 glazing.

Table 9
Rimini - Detailed comparison between reference and optimal TC configuration for each orientation.

|	Cooling (kWh/m^2)		Heating (kWh/m^2)		Lighting (kWh/m^2)		Total (kWh/m^2)		*Total Energy saving*
	TC	Ref	TC	Ref	TC	Ref	TC	Ref	
North	24.5	31.2	24.0	23.1	25.9	22.9	74.4	77.2	3.6%
South	22.7	49.4	19.2	11.7	18.9	17.7	60.8	78.8	22.8%
West	23.3	51.2	33.6	26.4	18.8	17.6	75.7	95.2	20.4%
East	26.4	52.0	31.6	25.3	22.3	19.3	80.3	96.6	16.9%

Table 10
Dzierzoniow - Detailed comparison between reference and optimal TC configuration for each orientation.

	Cooling (kWh/m^2)		Heating (kWh/m^2)		Lighting (kWh/m^2)		Total (kWh/m^2)		Total Energy saving
	TC	Ref	TC	Ref	TC	Ref	TC	Ref	
North	8.6	12.1	47.1	45.1	27.0	24.4	82.7	81.6	−1.3%
South	10.8	17.0	25.9	21.3	19.3	18.7	56.0	57.0	1.8%
West	9.8	16.8	59.0	54.4	19.2	18.7	88.0	89.9	2.1%
East	14.7	25.1	46.9	41.9	22.0	20.7	83.6	87.7	4.7%

coating along with different concentration of W-doping. Initial test has been performed and W-doping with 0.2, 0.5 and 0.7 wt% showed a decrease in thermochromic transition at 51, 49 and 42 °C respectively (Fig. 11). It is thus expected that increasing W concentration will further decrease the transition temperature to room temperature.

To achieve such result, the coating was realized through sol-gel synthesis process by coating VO$_2$ precursor on a clean glass substrate followed by thermal annealing as described in detail previously in Section 2. The glass substrate is a clear quartz glass whose optical properties were measured as well and used as a baseline.

Given results obtained with W-doping process, the multilayer thermochromic coating should be prepared with a W-doping higher than 0.7 wt%. With this configuration it is possible to achieve the energy saving determined with the optimization process described in Section 4. The optimized modulation range can also be achieved by appropriately designing a multilayer thermochromic coating and particularly by balancing the interplay between transmittance and reflectance in the hot and the cold states. Other strategies to control temperature transition and modulation range include via epitaxial or internal strains, introduction of O$_2$ vacancies and controlling the degree of crystallinity by
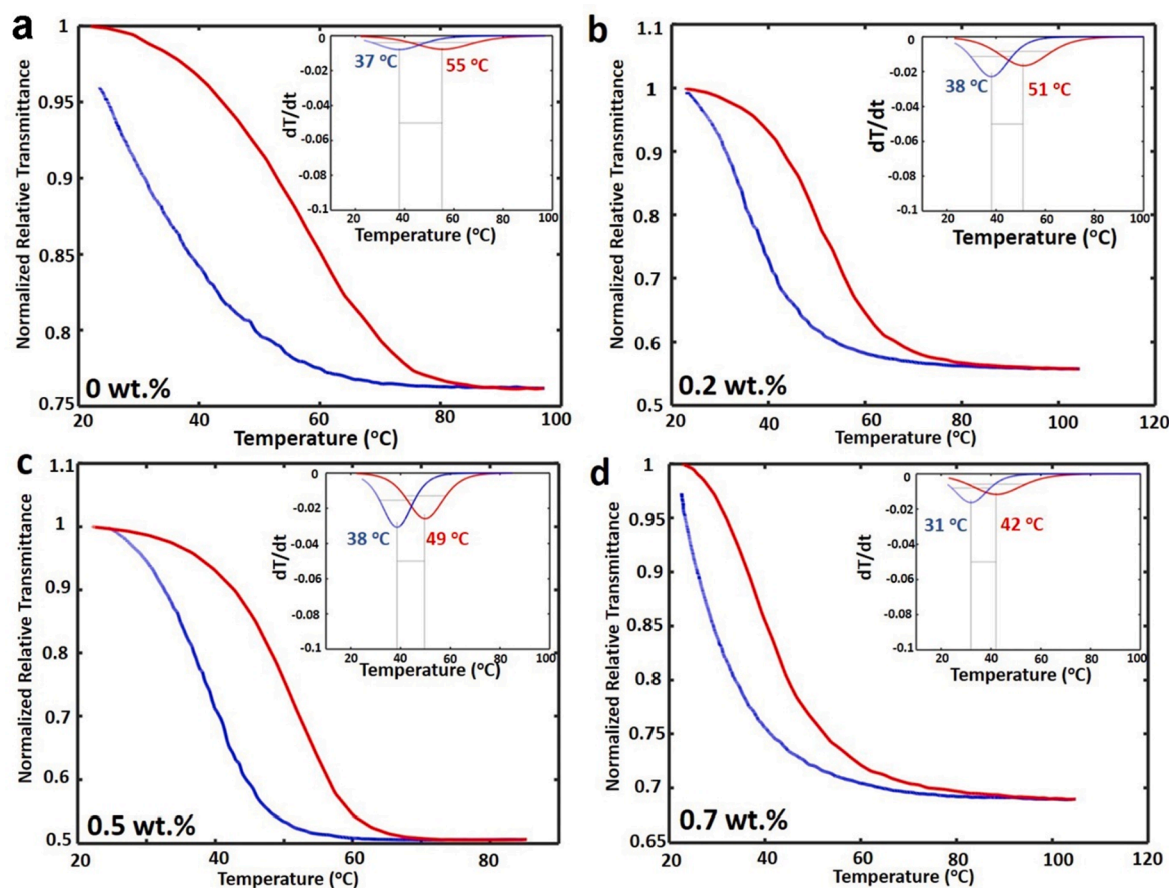
Fig. 11. Normalized Relative Transmission spectra of W-doped VO$_2$ samples with temperature (a-d) showing reduced transition temperature with increased doping. Inset in each figure shows corresponding first derivative of relative transmittance as a function of temperature.

carefully optimizing the annealing step.

Finally, the proposed guidelines were derived from the results that refer to a specific case study and climate zones. In addition, the simulation procedure involved a limited number of possible variation steps with specific maximum and minimum values for the climates under investigation. For a more general application of the proposed methodology, an optimization algorithm is under development able to work with larger ranges and smaller variation steps of the input parameters. The optimization should include also the economic features to support the identification of a thermochromic design that provide the balance between energy performances and costs. A key aspect of the thermochromic technology is its duration, that could degrade with time. An investigation of the coating durability is under progress with the use of natural and accelerated tests. Results from those tests will feed the optimization procedure for a more reliable economic analysis.

6. Conclusions

The research activity presented in this paper deals with the measurement and design optimization of the thermochromic layer in conjunction with a VIG glazing system. The activity is part of the EEN-SULATE project, aimed at developing a high performing system for glazed façade. The thermochromic thin-film was produced through sol-gel synthesis process by coating VO$_2$. Its optical properties were measured with a customized spectrophotometer to take into account temperature variations. A virtual mock-up, based on EnergyPlus engine, was created to assess the impact of the thermochromic layer on building's energy consumption. The thermochromic glazing was modelled and applied to the windowed wall of the mock-up. The thermochromic glazing was parametrized and different switching curves were created and used to predict the impact on the energy consumption for each orientation of the glazed wall in buildings located in two different climate zones (Italy and Poland). The results turned out to provide a significant impact for the Italian demo case. The optimal configuration should have a transition range of transmittance between 10 and 50%, with a fast transition around 25 °C. With those properties, the total energy consumption could be reduced up to 22.8% for the South orientation. Different results were found for the Polish demo case, where the reduced solar gain of winter was scarcely compensated by the cooling energy reduction. In fact, the application of the thermochromic layer registered as best performance an energy saving of 4.7% for the east orientation. The TC layer produces a decrease of the solar transmittance in comparison to the clear VIG, that causes a reduction of the cooling energy but also a reduction of the overall solar free gains in cold seasons. For this reason, the application to the Polish demo case showed a limited energy saving. So, the application of the TC film should be evaluated considering its application costs, that in some cases could be higher than the energy cost saving.

The experience presented in this paper shows that the proposed workflow could be used for the optimal design of the glazing system. Future developments are under evaluation concerning the experimental and numerical activities.

Declaration of Competing Interest

We declare no conflict of interest.

Acknowledgement

References

Aburas, M., Soebarto, V., Williamson, T., Liang, R., Ebendorff-Heidepriem, H., Wu, Y., 2019. Thermochromic smart window technologies for building application: A review. Appl. Energy 255, 113522. https://doi.org/10.1016/j.apenergy.2019.113522.

ASHRAE Handbook: Fundamentals, 2005. Atlanta.

ASTM E903-12, Standard Test Method for Solar Absorptance, Reflectance, and Transmittance of Materials Using Integrating Spheres, 2012.

ASTM G173-03 reference spectra, 2013.

Barron, S.C., Gorham, J.M., Patel, M.P., Green, M.L., 2014. High-throughput measurements of thermochromic behavior in V1- xNbxO2 combinatorial thin film libraries. ACS Comb. Sci. 16, 526–534. https://doi.org/10.1021/co500064p.

Barron, S.C., Patel, M.P., Nguyen, N., Nguyen, N.V., Green, M.L., 2015. An apparatus for spatially resolved, temperature dependent reflectance measurements for identifying thermochromism in combinatorial thin film libraries. Rev. Sci. Instrum. 86 https://doi.org/10.1063/1.4935477.

Berglund, C.N., Guggenheim, H.J., 1969. Electronic Properties of VO2 near the Semiconductor-Metal Transition. Phys. Rev. 185, 1022–1033. https://doi.org/10.1103/PhysRev.185.1022.

Bianco, L., Cascone, Y., Goia, F., Perino, M., Serra, V., 2017a. Responsive glazing systems: Characterisation methods and winter performance. Sol. Energy 155, 372–387. https://doi.org/10.1016/j.solener.2017.06.029.

Bianco, L., Cascone, Y., Goia, F., Perino, M., Serra, V., 2017b. Responsive glazing systems: Characterisation methods, summer performance and implications on thermal comfort. Sol. Energy 158, 819–836. https://doi.org/10.1016/j.solener.2017.09.050.

Costanzo, V., Evola, G., Marletta, L., 2016. Thermal and visual performance of real and theoretical thermochromic glazing solutions for office buildings. Sol. Energy Mater. Sol. Cells 149, 110–120. https://doi.org/10.1016/j.solmat.2016.01.008.

Cui, Y., Ke, Y., Liu, C., Chen, Z., Wang, N., Zhang, L., Zhou, Y., Wang, S., Gao, Y., Long, Y., 2018. Thermochromic VO2 for Energy-Efficient Smart Windows. Joule. https://doi.org/10.1016/j.joule.2018.06.018.

Eensulate [WWW Document], n.d. URL http://www.eensulate.eu/ (accessed 8.10.20).

EnergyPlus [WWW Document], n.d. URL https://energyplus.net/ (accessed 8.10.20).

Fazel, A., Izadi, A., Azizi, M., 2016. Low-cost solar thermal based adaptive window: Combination of energy-saving and self-adjustment in buildings. Sol. Energy 133, 274–282. https://doi.org/10.1016/j.solener.2016.04.008.

Gao, Y., Luo, H., Zhang, Z., Kang, L., Chen, Z., Du, J., Kanehira, M., Cao, C., 2012. Nanoceramic VO 2 thermochromic smart glass: A review on progress in solution processing. Nano Energy 1, 221–246. https://doi.org/10.1016/j.nanoen.2011.12.002.

Giovannini, L., Favoino, F., Pellegrino, A., Lo Verso, V.R.M., Serra, V., Zinzi, M., 2019. Thermochromic glazing performance: From component experimental characterisation to whole building performance evaluation. Appl. Energy 251, 113335. https://doi.org/10.1016/j.apenergy.2019.113335.

Hee, W.J., Alghoul, M.A., Bakhtyar, B., Elayeb, O., Shameri, M.A., Alrubaih, M.S., Sopian, K., 2015. The role of window glazing on daylighting and energy saving in buildings. Renew. Sustain. Energy Rev. https://doi.org/10.1016/j.rser.2014.09.020.

Imbert, P., Larsen, O.K., Johra, H., 2019. Study of thermochromic glass performance in the Danish climate and visual comfort perspectives. J. Phys. Conf. Ser. 1343 https://doi.org/10.1088/1742-6596/1343/1/012197.

Intergovernmental Panel on Climate Change, 2014. Climate Change 2014 Mitigation of Climate Change, Climate Change 2014 Mitigation of Climate Change. Cambridge University Press. https://doi.org/10.1017/cbo9781107415416.

Kottek, M., Grieser, J., Beck, C., Rudolf, B., Rubel, F., 2006. World Map of the Köppen-Geiger climate classification updated 15, 259–263. https://doi.org/10.1127/0941-2948/2006/0130.

Kuhn, T.E., 2017. State of the art of advanced solar control devices for buildings. Sol. Energy 154, 112–133. https://doi.org/10.1016/j.solener.2016.12.044.

Long, L., Ye, H., 2014a. How to be smart and energy efficient: A general discussion on thermochromic windows. Sci. Rep. 4, 1–10. https://doi.org/10.1038/srep06427.

Long, L., Ye, H., 2014b. Discussion of the performance improvement of thermochromic smart glazing applied in passive buildings. Sol. Energy 107, 236–244. https://doi.org/10.1016/j.solener.2014.05.014.

Long, L., Ye, H., Zhang, H., Gao, Y., 2015. Performance demonstration and simulation of thermochromic double glazing in building applications. Sol. Energy 120, 55–64. https://doi.org/10.1016/j.solener.2015.07.025.

Raicu, A., Wilson, H.R., Nitz, P., Platzer, W., Wittwer, V., Jahns, E., 2002. Facade systems with variable solar control using thermotropic polymer blends. Sol. Energy 72, 31–42. https://doi.org/10.1016/S0038-092X(01)00093-7.

Riffat, S.B., Mardiana, A., 2015. Building Energy Consumption and Carbon dioxide Emissions: Threat to Climate Change. J. Earth Sci. Clim. Change s3. https://doi.org/10.4172/2157-7617.s3-001.

Saeli, M., Piccirillo, C., Parkin, I.P., Binions, R., Ridley, I., 2010. Energy modelling studies of thermochromic glazing. Energy Build. 42, 1666–1673. https://doi.org/10.1016/j.enbuild.2010.04.010.

Salamati, M., Kamyabjou, G., Mohamadi, M., Taghizade, K., Kowsari, E., 2019. Preparation of TiO2@W-VO2 thermochromic thin film for the application of energy efficient smart windows and energy modeling studies of the produced glass. Constr. Build. Mater. 218, 477–482. https://doi.org/10.1016/j.conbuildmat.2019.05.046.

Santamouris, M., 2014. Cooling the cities - A review of reflective and green roof mitigation technologies to fight heat island and improve comfort in urban environments. Sol. Energy 103, 682–703. https://doi.org/10.1016/j.solener.2012.07.003.

Shvets, P., Dikaya, O., Maksimova, K., Goikhman, A., 2019. A review of Raman spectroscopy of vanadium oxides. J. Raman Spectrosc. 50, 1226–1244. https://doi.org/10.1002/jrs.5616.

Smith, T., Guild, J., 1931. The C.I.E. colorimetric standards and their use. Trans. Opt. Soc. https://doi.org/10.1088/1475-4878/33/3/301.

Sol, C., Portnoi, M., Li, T., Gurunatha, K.L., Schläfer, J., Guldin, S., Parkin, I.P., Papakonstantinou, I., 2020. High-Performance Planar Thin Film Thermochromic Window via Dynamic Optical Impedance Matching. ACS Appl. Mater. Interfaces 12, 8140–8145. https://doi.org/10.1021/acsami.9b18920.

Tällberg, R., Jelle, B.P., Loonen, R., Gao, T., Hamdy, M., 2019. Comparison of the energy saving potential of adaptive and controllable smart windows: A state-of-the-art review and simulation studies of thermochromic, photochromic and electrochromic technologies. Sol. Energy Mater. Sol. Cells 200, 109828. https://doi.org/10.1016/j.solmat.2019.02.041.

Taylor, A., Parkin, I., Noor, N., Tummeltshammer, C., Brown, M.S., Papakonstantinou, I., 2013. A bioinspired solution for spectrally selective thermochromic VO_2 coated intelligent glazing. Opt. Express 21, A750. https://doi.org/10.1364/oe.21.00a750.

Warwick, M.E.A., Ridley, I., Binions, R., 2016. Variation of thermochromic glazing systems transition temperature, hysteresis gradient and width effect on energy efficiency. Buildings 6. https://doi.org/10.3390/buildings6020022.